Journal of Applied Analysis and Computation
Volume 12, Number 4, August 2022, 1517–1531
Website:http://www.jaac-online.com
DOI:10.11948/20210317

BIFURCATIONS AND EXACT SOLUTIONS OF THE OPTICAL SOLITON MODEL IN METAMATERIALS DOMINATED BY ANTI-CUBIC NONLINEARITY*

Qiuyan Zhang[1,†]

Abstract Optical soliton model in metamaterials, dominanted by anti-cubic nonlinearity, is investigated by the method of dynamical systems. By using travelling wave transformation, the model can be converted into a singular integrable travelling wave system. Then we discuss the dynamical behavior of the associated regular system. Further, all bounded exact solutions of the model can be calculated because of its integrability. Finally, twenty exact explicit parametric representations are derived.

Keywords Bifurcation, homoclinic orbit, heteroclinic orbit, periodic peakon, optical soliton model.

MSC(2010) 34C23, 34C25, 34C37, 74J30.

1. Introduction

Optical metamaterials have become one of the attractive research topics in the context of optical fibers. There are many results obtained in the study of optical solitons in nonlinear meatamaterials (see [10, 12, 16, 17, 19–25]). The propagation of pulses in nonlinear metamaterials can be described by the form of the nonlinear Schrödinger equation. Some forms of nonlinearity have been addressed in this context, such as non-kerr law, self-steepening and nonlinear dispersion. Various kinds of non-kerr laws include power law, parabolic law, dual-power law, saturating law, exponential law, log law, triple-power law and so on. If the dominant non-kerr law effect is considered to be in the form of anti-cubic type and Hamiltonian perturbation terms include inter-modal dispersion, self-steepening and nonlinear dispersion, the governing equation of this model has the form

$$\begin{aligned} &iq_t + aq_{xx} + (b_1|q|^{-4} + b_2|q|^2 + b_3|q|^4)q \\ =&i[\alpha q_x + \beta(|q|^2q)_x + \gamma(|q|^2)_xq] + \theta_1(|q|^2q)_{xx} + \theta_2|q|^2q_{xx} + \theta_3q^2q^*_{xx}, \end{aligned} \tag{1.1}$$

where $q(x,t)$ represents the wave profile, which is a complex-valued function of the spatial variable x and the temporal variable t. * denotes complex conjugate. The

†The corresponding author. Email address: zqy1607@cuit.edu.cn(Q. Zhang)
[1]College of Applied Mathematics, Chengdu University of Information Technology, No.24, Section 1, Xuefu Road, Southwest Airport Economic Development Zone, Chengdu 610225, China
*The author was supported by National Natural Science Foundation of China (12101090) and Sichuan Science and Technology Program (2021ZYD0009).

first two terms on the left of equation (1.1) account for the temporal evolution and the group velocity dispersion.The next three terms stand for the nonlinear influence of non-Kerr law, where b_1-term introduces the anti-cubic effect and other two b_i-terms account for parabolic effect. The right of equation (1.1) are the Hamiltonian perturbation terms. The perturbation terms with α, β and γ denote inter-modal dispersion, self-steepening and nonlinear dispersion, respectively. The remaining three perturbation terms with θ_i $(i = 1, 2, 3)$ arise from optical metamaterials.

Equation (1.1) is a generalization of the model that was reported and studied earlier in [3]. It has been considered by many authors using different integration methods. In [4] and [5], Biswas et al. considered equation (1.1) in the case $b_2 = b_3 = 0$ and obtained bright, dark and singular 1-soliton solution using the ansatz approach and the simplest equation approach. Afzal et al. discussed equation (1.1) for $\alpha = \beta = \gamma = \theta_i = 0$ in [1] and gave the constraint conditions for the existence of optical dark and dark-singular solitons. Kader et al. studied the case $3\theta_1 - \theta_2 - \theta_3 = 0$ using the Lie group method and obtained the explicit forms for dark and bright soliton solutions and the Jacobian elliptic function forms for the doubly periodic solutions in [11]. For $\theta_1 = 0$ and $\theta_2 + \theta_3 = 0$, Foroutan et al. applied the extended trial equation, the improved G'/G-expansion method in [8] and the improved $tan(\phi(\xi)/2)$-expansion method in [9] and retrieved bright, dark and singular soliton solutions. Ekici et al. also considered the case using the extended trial equation method and obtained bright and singular solitons in [7]. Al-Ghafai and Krishnan [2] still analyzed the case and applied four integration schemes, namely, the projective Riccati equations method, the new auxiliary equation method the new mapping method and the Bernoulli sub-ODE method, and obtained various types of exact soliton solutions and some other solutions such as trigonometric solutions, Jacobian elliptic solutions and rational solutions. However, the obtained results are still incomplete.

In this paper, by using dynamical system method, we consider the solutions of equation (1.1) having the form

$$q(x,t) = \phi(\xi)e^{-i(\kappa x - \omega t)}, \quad \xi = x - vt. \tag{1.2}$$

Substituting (1.2) into (1.1) and separating the real and imaginary parts, we have

$$[a - (3\theta_1 + \theta_2 + \theta_3)\phi^2]\phi'' - \lambda\phi + b_1\phi^{-3} + \sigma\phi^3 + b_3\phi^5 - 6\theta_1\phi(\phi')^2 = 0, \tag{1.3}$$

$$(v + \alpha + 2a\kappa) + [3\beta + 2\gamma - 2\kappa(3\theta_1 + \theta_2 - \theta_3)]\phi^2 = 0, \tag{1.4}$$

where $\lambda = \omega + \alpha\kappa + a\kappa^2, \sigma = b_2 - \kappa\beta + (\theta_1 + \theta_2 + \theta_3)\kappa^2$, the notation $\phi' = \frac{d\phi}{d\xi}$. From the imaginary part equation (1.4), upon setting the coefficients of linearly independent functions to zero gives the relations:

$$v = -(\alpha + 2a\kappa), \quad 3\beta + 2\gamma = 2\kappa(3\theta_1 + \theta_2 - \theta_3). \tag{1.5}$$

Similar to [2], in this paper, we assume that $\theta_1 = 0$ and $\theta_2 + \theta_3 = 0$. In this case, we see from (1.5) that

$$\lambda = \frac{\gamma^2 - \alpha^2 + 4a\omega}{4a}, \quad \sigma = \frac{2ab_2 + \alpha\beta + \beta\gamma}{2a}, \quad \theta_2 = -\frac{a(3\beta + 2\gamma)}{2(\alpha + v)}. \tag{1.6}$$

Equation (1.3) reduces to

$$a\phi'' - \lambda\phi + b_1\phi^{-3} + \sigma\phi^3 + b_3\phi^5 = 0.$$

which is equivalent to the planar dynamical system

$$\frac{d\phi}{d\xi} = y, \quad \frac{dy}{d\xi} = \frac{-b_1 + \lambda\phi^4 - \sigma\phi^6 - b_3\phi^8}{a\phi^3}. \tag{1.7}$$

System (1.7) has the first integral for $a \neq 0$

$$H_1(\phi, y) = y^2 + \frac{1}{a}\left(\frac{1}{3}b_3\phi^6 + \frac{1}{2}\sigma\phi^4 - \lambda\phi^2 - \frac{b_1}{\phi^2}\right) = h. \tag{1.8}$$

Clearly, system (1.7) with $a \neq 0$ are the singular nonlinear traveling wave system of the first class defined in [13, 14] and [15]. It is very interesting that singular traveling systems have peakon, pseudo-peakon, periodic peakon and compacton solution families. Periodic peakons are classical solutions with two time scales of a singular traveling system. Peakon is a limit solution of a family of periodic peakons or a limit solution of family of pseudo-peakons under two classes of limit senses (see [18]). Compacton family is a solution family of system (1.4) for which all solutions $\phi(\xi)$ have finite support set, i.e., the defined region of every $\phi(\xi)$ with respect to ξ is finite and the value region of ϕ is bounded. Corresponding to different types of phase orbits, in [13,14] and [15], the authors gave rise to a classification for different wave profiles of $\phi(\xi)$. For system (1.7), we use the method of dynamical systems to investigate their dynamical behavior and to find all possible exact explicit parametric representations for all bounded solutions $\phi(\xi)$ of the systems.

This paper is organized as follows. For a fixed $a > 0$ and varying b_1, in section 2, we discuss bifurcations of phase portraits of system (1.7) and exact solutions when $\gamma^2 - \alpha^2 + 4a\omega < 0, 2ab_2 + \alpha\beta + \beta\gamma > 0$ and $b_3 < 0$. In section 3, we consider the same problems of system (1.7) under the parameter condition $\gamma^2 - \alpha^2 + 4a\omega > 0, 2ab_2 + \alpha\beta + \beta\gamma < 0$ and $b_3 > 0$.

The main result of this paper is the following theorem, which can be proved in next two sections.

Theorem 1.1. *Assume that the parameters in equation* (1.1) *satisfy* $\theta_1 = 0, \theta_2 + \theta_3 = 0$. *For a fixed* $a > 0$, *the following conclusions hold.*

(1) When $\gamma^2 - \alpha^2 + 4a\omega < 0, 2ab_2 + \alpha\beta + \beta\gamma < 0$ *and* $b_3 > 0$, *the travelling wave system* (1.7) *of equation* (1.1) *has the phase portraits as shown in Fig.1. Equation* (1.1) *has the exact explicit solutions with the form* (1.2) *and* $\phi(\xi)s$ *are given by* (2.6)-(2.16).

(2) When $\gamma^2 - \alpha^2 + 4a\omega > 0, 2ab_2 + \alpha\beta + \beta\gamma > 0$ *and* $b_3 < 0$, *the travelling wave system* (1.7) *of equation* (1.1) *has the phase portraits as shown in Fig.4. Equation* (1.1) *has the exact explicit solutions with the form* (1.2) *and* $\phi(\xi)s$ *are given by* (3.2)-(3.10).

2. Case I: $a > 0, \gamma^2 - \alpha^2 + 4a\omega < 0, 2ab_2 + \alpha\beta + \beta\gamma < 0, b_3 > 0$

In this section, we consider bifurcations of phase portraits of system (1.7) depending on the parameter group $(a, \lambda, b_1, \sigma, b_3)$, where λ and σ are defined by (1.6). We study the associated regular system of system (1.7) as follows:

$$\frac{d\phi}{d\zeta} = ay\phi^3, \quad \frac{dy}{d\zeta} = -b_1 + \phi^4(\lambda - \sigma\phi^2 - b_3\phi^4), \tag{2.1}$$

where $d\xi = a\phi^3 d\zeta$, for $\phi \neq 0$. System (2.1) has the same first integral as (1.7). But the vector fields defined by system (1.7) and system (2.1) are different (see [13] and [17]).

2.1. Phase portraits of system (1.7) for Case I

Assume that $\gamma^2 - \alpha^2 + 4a\omega < 0, 2ab_2 + \alpha\beta + \beta\gamma < 0, b_3 > 0$, it is equivalent to that $a > 0, \lambda < 0, \sigma < 0, b_3 > 0$.

Write that $F(\phi) := -b_1 + \phi^4 F_4(\phi), F_4(\phi) := \lambda - \sigma\phi^2 - b_3\phi^4$, then $F'(\phi) = \phi^3(4\lambda - 6\sigma\phi^2 - 8b_3\phi^4)$. We always assume that $b_1 \neq 0$ and $\Delta := \sigma^2 + 4\lambda b_3 > 0$. Because function $F(\phi)$ is an even function of ϕ, to investigate the equilibrium points of system (2.1), we only need to discuss the positive real zeros of function $F(\phi)$. Under mentioned parameter conditions, we know that $F(-\infty) = F(\infty) = -\infty, F(0) = -b_1$ and $F'(\hat{\phi}_{1,2}) = 0$, where $\hat{\phi}_1 = \frac{1}{2}\left(-\frac{\sqrt{\Delta_1}+3\sigma}{2b_3}\right)^{\frac{1}{2}}$, $\hat{\phi}_2 = \frac{1}{2}\left(\frac{\sqrt{\Delta_1}-3\sigma}{2b_3}\right)^{\frac{1}{2}}$ and $\Delta_1 = 9\sigma^2 + 32b_1b_3$. Denote that

$$F_4^m := \hat{\phi}_1^4 F_4(\hat{\phi}_1) = \frac{(3\sigma + \sqrt{\Delta_1})^2(3\sigma^2 + 16\lambda b_3 + \sigma\sqrt{\Delta_1})}{2048b_3^3}. \tag{2.2}$$

$$F_4^M := \hat{\phi}_2^4 F_4(\hat{\phi}_2) = \frac{(-3\sigma + \sqrt{\Delta_1})^2(-3\sigma^2 - 16\lambda b_3 + \sigma\sqrt{\Delta_1})}{2048b_3^3}. \tag{2.3}$$

$$\hat{b}_1 := -\phi_1^2\phi_3^2\big[\frac{1}{3}b_3(\phi_1^4 + \phi_1^2\phi_3^2 + \phi_3^2) + \frac{1}{2}\sigma(\phi_1^2 + \phi_3^2) - \lambda\big]. \tag{2.4}$$

It is easy to obtain that the following conclusion hold.

(i) When $b_1 < F_4^m$, the function $F(\phi)$ has only one simple positive zero ϕ_3.

(ii) When $b_1 = F_4^m$, the function $F(\phi)$ has a simple positive real zero ϕ_3 and one double positive real zero $\phi_1 = \phi_2$.

(iii) When $F_4^m < b_1 < 0$, the function $F(\phi)$ has three simple positive real zeros $\phi_j, j = 1, 2, 3$. In addition, if $b_1 = \hat{b}_1 < 0$, we have $H_1(\phi_1, 0) = H_1(\phi_3, 0)$.

(iv) When $b_1 = 0$, $\phi_1 = 0$ is the zero of the function $F(\phi)$ and there exist two other simple positive real zeros.

(v) When $0 < b_1 < F_4^M$, the function $F(\phi)$ has two simple positive real zeros $\phi_j, j = 1, 2$.

(vi) When $b_1 = F_4^M$, the function $F(\phi)$ has a double positive real zero $\phi_2 = \phi_3$.

Let $M(\phi_j, 0)$ be the coefficient matrix of the linearized system of system (2.1) at an equilibrium point $E_j(\phi_j, y_j)$ and $J(\phi_j, y_j) = \mathrm{detM}(\phi_j, y_j)$. We have $J(\phi_j, 0) = -a\phi_j^3 F'(\phi_j)$. By the theory of planar dynamical systems (see [13]), for an equilibrium point of a planar integrable system, if $J < 0$, then the equilibrium point is a saddle point; If $J > 0$ and $(\mathrm{Trace}M)^2 - 4J < 0 (> 0)$, then it is a center point (a node point); If $J = 0$ and the Poincaré index of the equilibrium point is equal to zero, then the equilibrium point is a cusp.

Write that $h_j = H_1(\phi_j, 0)$, where $H_1(\phi, y)$ is defined by (1.8). For a fixed parameter group $a > 0, \lambda < 0, \sigma < 0, b_3 > 0$, by varying the parameter b_1, and using the above information to do qualitative analysis, we have the following bifurcations of the phase portraits of system (1.7) as shown in Fig.1. It should be noted that we take fixed parameter group: $(a, \lambda, \sigma, b_3) = (1, -7.8, -3.9, 0.45)$ in Fig.1. In this case, $F_4^m = -7.27571243, F_4^M = 13.0850874, \hat{b}_1 = -3.5645$.

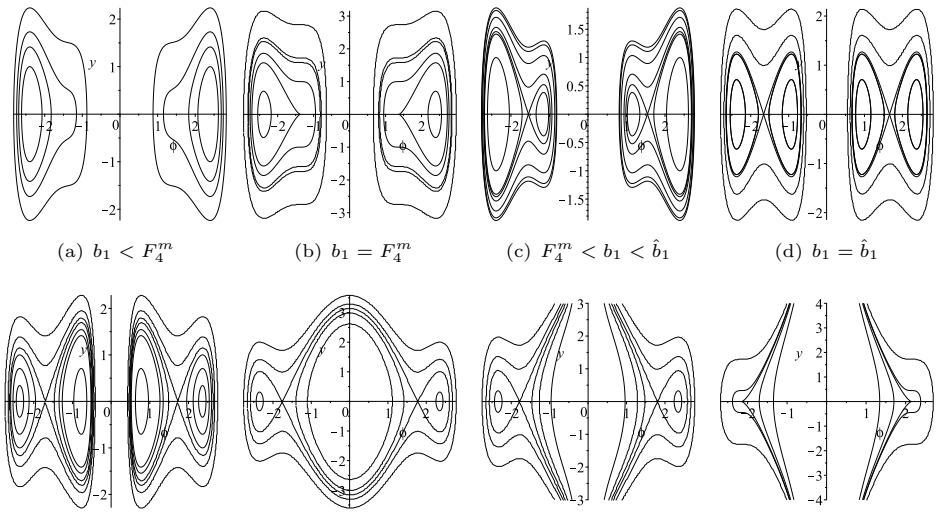

(a) $b_1 < F_4^m$ (b) $b_1 = F_4^m$ (c) $F_4^m < b_1 < \hat{b}_1$ (d) $b_1 = \hat{b}_1$

(e) $\hat{b}_1 < b_1 < 0$ (f) $b_1 = 0$ (g) $0 < b_1 < F_4^M$ (h) $b_1 = F_4^M$

Figure 1. The bifurcations of phase portraits of system (1.7) as b_1 is varied.

2.2. Exact parametric representations of the orbits given by Fig.1

We see from (1.8) that

$$y^2 = \frac{1}{\phi^2}\left(h\phi^2 - \frac{1}{a}\left(\frac{1}{3}b_3\phi^8 + \frac{1}{2}\hat{b_2}\phi^6 - \lambda\phi^4 + b_1\right)\right)$$
$$= \frac{b_3}{3a\phi^2}\left(-\frac{3b_1}{b_3} + \frac{3ah}{b_3}\phi^2 + \frac{3\lambda}{b_3}\phi^4 - \frac{3\sigma}{2b_3}\phi^6 - \phi^8\right).$$

Thus, by using the first equation of system (1.7), we have

$$\omega_0\xi \equiv \sqrt{\frac{4b_3}{3a}}\xi = \int_{\psi_0}^{\psi} \frac{d\psi}{\sqrt{-\frac{3b_1}{b_3} + \frac{3ah}{b_3}\psi + \frac{3\lambda}{b_3}\psi^2 - \frac{3\sigma}{2b_3}\psi^3 - \psi^4}}, \tag{2.5}$$

where $\psi = \phi^2$. Applying (2.5), we can calculate the exact parametric representations of the orbits given by Fig.1.

(i) Fig.1 (a). In this case, in the right phase plane, system (1.7) has only one positive equilibrium point $E_3(\phi_3, 0)$.

Corresponding to the right family of closed orbits defined by $H_1(\phi, y) = h, h \in (h_3, \infty)$, enclosing the left equilibrium point $E_3(\phi_3, 0)$ in Fig.1 (a), (2.5) has the form

$$\omega_0\xi = \int_{\psi_b}^{\psi} \frac{d\psi}{(\sqrt{(\psi_a - \psi)(\psi - \psi_b)[(\psi - \tilde{b}_1)^2 + \tilde{a}_1^2]}}.$$

It gives rise to the following periodic solution family of system (1.7):

$$\phi(\xi) = \left(\breve{\alpha}_1 + \frac{\breve{\beta}_1}{1 + \hat{\alpha}_1 \mathrm{cn}(\Omega_1\xi, k)}\right)^{\frac{1}{2}}, \tag{2.6}$$

where $\mathrm{cn}(\cdot,k)$ is the Jacobian elliptic function (see [6]), $\breve{\alpha}_1 = \frac{\psi_a B_1 - \psi_b A_1}{B_1 - A_1}, \breve{\beta}_1 = \frac{2A_1B_1(1-\psi_b)}{A_1^2 - B_1^2}, \hat{\alpha}_1 = \frac{A_1 - B_1}{A_1 + B_1}, \Omega_1 = \omega_0\sqrt{A_1B_1}, k^2 = \frac{(\psi_a - \psi_b)^2 - (A_1 - B_1)^2}{4A_1B_1}, A_1^2 = (\psi_a - \tilde{b}_1)^2 + \tilde{b}_1^2$ and $B_1^2 = (\psi_b - \tilde{b}_1)^2 + \tilde{a}_1^2$.

(ii) Fig.1 (b). In this case, we have $\phi_1 = \phi_2, h_1 = h_2$.

Corresponding to the right family of closed orbits defined by $H_1(\phi, y) = h, h \in (h_3, h_2)$, enclosing the right equilibrium point $E_3(\phi_3, 0)$ in Fig.1 (b), it has the same parametric representation as (2.6).

Corresponding to the right homoclinic orbit to the cusp equilibrium point $E_1(\phi_1,0)$ defined by $H_1(\phi, y) = h_1 = h_2$, now (2.5) can be written as

$$\omega_0 \xi = \int_{\psi}^{\psi_M} \frac{d\psi}{(\psi - \psi_1)\sqrt{(\psi_M - \psi)(\psi - \psi_1)}}.$$

Hence, it follows the solitary wave solution as follows:

$$\phi(\xi) = \left(\psi_1 + \frac{4(\psi_M - \psi_1)}{4 + (\psi_M - \psi_1)^2 \omega_0^2 \xi^2}\right)^{\frac{1}{2}}, \tag{2.7}$$

where $\psi_1 = \phi_1^2$ and $\psi_M = \phi_M^2$.

Corresponding to the right family of closed orbits defined by $H_1(\phi, y) = h, h \in (h_1, \infty)$, enclosing the right equilibrium points $E_1(\phi_1, 0)$ and $E_3(\phi_3, 0)$ in Fig.1 (b), it has the same parametric representation as (2.6).

(iii) Fig.1 (c). In this case, we have $h_3 < h_1 < h_2$. With h is varied, the changes of level curves defined by $H_1(\phi, y) = h$ are shown in Fig.2 (a)-(d).

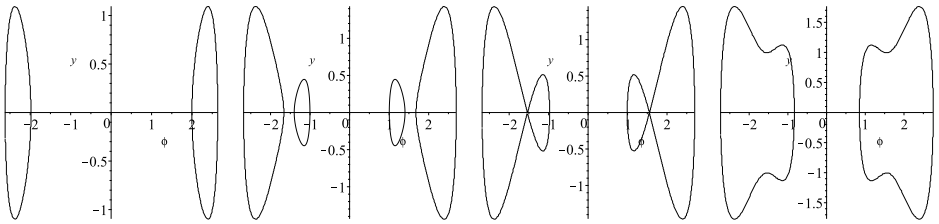

(a) $h_3 < h \leq h_1$ (b) $h_1 < h < h_2$ (c) $h = h_2$ (d) $h > h_2$

Figure 2. The level curves $H_1(\phi, y) = h$ of system (1.7) as h is varied for $h_3 < h_1 < h_2$

Corresponding to the right family of closed orbits defined by $H_1(\phi, y) = h, h \in (h_3, h_1)$, enclosing the right equilibrium point $E_3(\phi_3, 0)$ in Fig.2 (a), it has the same parametric representation as (2.6).

Corresponding to the right two families of closed orbits defined by $H_1(\phi, y) = h, h \in (h_1, h_3)$, enclosing the right equilibrium points $E_3(\phi_3, 0)$ and $E_1(\phi_1, 0)$, respectively, in Fig.2 (b), (2.5) has forms

$$\omega_0 \xi = \int_{\psi_b}^{\psi} \frac{d\psi}{(\sqrt{(\psi_a - \psi)(\psi - \psi_b)[(\psi - \psi_c)(\psi - \psi_d)}}$$

and

$$\omega_0 \xi = \int_{\psi_d}^{\psi} \frac{d\psi}{(\sqrt{(\psi_a - \psi)(\psi_b - \psi)[(\psi_c - \psi)(\psi - \psi_d)}}.$$

Therefore, the family of closed orbits enclosing the right equilibrium points $E_3(\phi_3, 0)$ has the parametric representation:

$$\phi(\xi) = \left(\psi_c + \frac{\psi_b - \psi_c}{1 - \hat{\alpha}_3^2 \mathrm{sn}^2(\Omega_2 \xi, k)}\right)^{\frac{1}{2}}, \tag{2.8}$$

where $\mathrm{sn}(\cdot, k)$ is the Jacobian elliptic function (see [6]), $\hat{\alpha}_3^2 = \frac{\psi_a - \psi_b}{\psi_a - \psi_b}$, $k^2 = \frac{\hat{\alpha}_3^2(\psi_c - \psi_d)}{\psi_b - \psi_d}$ and $\Omega_2 = \frac{1}{2}\omega_0\sqrt{(\psi_a - \psi_c)(\psi_b - \psi_d)}$.

The family of closed orbits enclosing the right equilibrium points $E_1(\phi_1, 0)$ has the parametric representation:

$$\phi(\xi) = \left(\psi_a - \frac{\psi_a - \psi_d}{1 - \hat{\alpha}_4^2 \mathrm{sn}^2(\Omega_3 \xi, k)}\right)^{\frac{1}{2}}, \tag{2.9}$$

where $\hat{\alpha}_4^2 = \frac{\psi_d - \psi_c}{\psi_a - \psi_c} < 0, \Omega_3 = \frac{1}{2}\omega_0\sqrt{(\psi_a - \psi_c)(\psi_b - \psi_d)}$ and $k^2 = \frac{-\hat{\alpha}_4^2(\psi_a - \psi_b)}{\psi_b - \psi_d}$.

Corresponding to the right two homoclinic orbits (see Fig.2(c)) to the equilibrium point $E_2(\phi_2, 0)$ defined by $H_1(\phi, y) = h_2$, enclosing the right equilibrium points $E_1(\phi_1, 0)$ and $E_3(\phi_3, 0)$, respectively, now (2.5) can be written as $\omega_0\xi = \int_{\psi}^{\psi_M} \frac{d\psi}{(\psi - \psi_2)\sqrt{(\psi_M - \psi)(\psi - \psi_m)}}$ and $\omega_0\xi = \int_{\psi_m}^{\psi} \frac{d\psi}{(\psi_2 - \psi)\sqrt{(\psi_M - \psi)(\psi - \psi_m)}}$. Hence, we obtain the following two parametric representations:

$$\phi(\xi) = \left(\psi_2 - \frac{2(\psi_M - \psi_2)(\psi_2 - \psi_m)}{(\psi_M - \psi_m)\cosh\left(\omega_0\sqrt{(\psi_M - \psi_2)(\psi_2 - \psi_m)}\xi\right) + (\psi_M + \psi_m - 2\psi_2)}\right)^{\frac{1}{2}} \tag{2.10}$$

and

$$\phi(\xi) = \left(\psi_2 + \frac{2(\psi_M - \psi_2)(\psi_2 - \psi_m)}{(\psi_M - \psi_m)\cosh\left(\omega_0\sqrt{(\psi_M - \psi_2)(\psi_2 - \psi_m)}\xi\right) - (\psi_M + \psi_m - 2\psi_2)}\right)^{\frac{1}{2}}. \tag{2.11}$$

Corresponding to the right global family (see Fig.2(d)) of closed orbits defined by $H_1(\phi, y) = h, h \in (h_2, \infty)$, enclosing the left three equilibrium points $E_j(\phi_j, 0), j = 1, 2, 3$, it has the same parametric representation as (2.6).

Notice that the family of global periodic orbits defined by $H_1(\phi, y) = h, h \in (h_2, \infty)$ gives rise to a family of periodic peakons (see Fig.3 (a)). The right homoclinic orbit defined by $H_1(\phi, y) = h_2$, enclosing the left equilibrium points $E_1(\phi_1, 0)$ gives rise to a anti-pseudo-peakon solution of system (1.7) (see Fig.3 (b)). Because these orbits are very close to the singular straight line $\phi = 0$.

(iv) Fig.1 (d). In this case, we have $h_1 = h_3$.

Corresponding to the right two families of closed orbits defined by $H_1(\phi, y) = h, h \in (h_1, h_2)$, enclosing the right equilibrium points $E_3(\phi_3, 0)$ and $E_1(\phi_1, 0)$, respectively, in Fig.1 (d), we have the same parametric representation as (2.8) and (2.9).

Corresponding to the right two homoclinic orbit to the equilibrium point $E_2(\phi_2,0)$ defined by $H_1(\phi, y) = h_2$, enclosing the right equilibrium points $E_1(\phi_1, 0)$ and $E_3(\phi_3, 0)$, respectively, now we have $\psi_M - \psi_2 = \psi_2 - \psi_m$. Thus, we get the following two parametric representations:

$$\phi(\xi) = (\psi_2 - (\psi_2 - \psi_m)\mathrm{sech}\,(\omega_0(\psi_M - \psi_2)\xi))^{\frac{1}{2}} \tag{2.12}$$

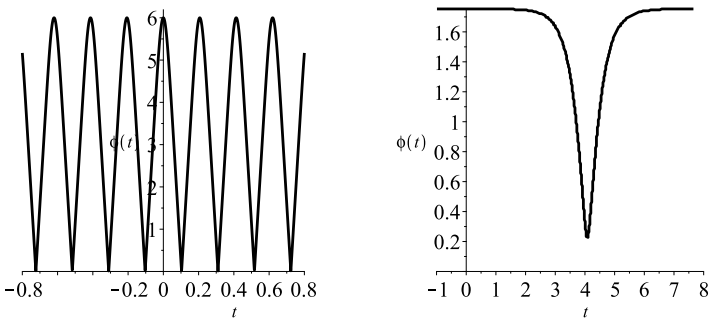

(a) Periodic peakon (b) Anti-pseudo-peakon

Figure 3. The profiles of the solution $\phi(\xi)$ of system (1.7)

and

$$\phi(\xi) = (\psi_2 + (\psi_M - \psi_2)\text{sech}\,(\omega_0(\psi_M - \psi_2)\xi))^{\frac{1}{2}}\,. \tag{2.13}$$

Corresponding to the right global family of closed orbits defined by $H_1(\phi, y) = h, h \in (h_2, \infty)$, enclosing the right three equilibrium points $E_j(\phi_j, 0), j = 1, 2, 3$ in Fig.1 (d), it has the same parametric representation as (2.6).

(v) Fig.1 (e). In this case, the parametric representations of all orbits of system (1.7) is similar to the case (iii).

(vi) Fig.1 (g). In this case, system (1.7) has two equilibrium points at the positive $\phi-$axis.

The level curves defined by $H_1(\phi, y) = h, h \in (h_2, h_1)$ in Fig.1 (g) contain two families of closed orbits enclosing the equilibrium points $E_2(\phi_2, 0)$ and $E_2'(-\phi_2, 0)$, and two open orbit families which tend to the singular straight line $\phi = 0$, respectively, when $|y| \to \infty$.

Corresponding to the right family of closed orbits enclosing the right equilibrium points $E_2(\phi_2, 0)$, (2.5) has the form $\omega_0\xi = \int_{\psi_b}^{\psi} \frac{d\psi}{\sqrt{\psi_a-\psi)(\psi-\psi_b)(\psi-\psi_c)(\psi+\psi_d)}}$. Thus, we obtain the following exact periodic solution family of system (1.7):

$$\phi(\xi) = \left(\psi_c + \frac{\psi_b - \psi_c}{1 - \hat{\alpha}_4^2 \text{sn}^2(\Omega_4\xi, k}\right)^{\frac{1}{2}}, \tag{2.14}$$

where $\hat{\alpha}_4^2 = \frac{\psi_a-\psi_b}{\psi_a-\psi_c}, \Omega_4 = \frac{1}{2}\omega_0\sqrt{(\psi_a - \psi_c)(\psi_b + \psi_d)}$ and $k^2 = \frac{\hat{\alpha}_4^2(\psi_d-\psi_c)}{\psi_b+\psi_d}$.

Corresponding to the right family of open orbit family, (2.5) has the form $\omega_0\xi = \int_{\psi}^{\psi_c} \frac{d\psi}{\sqrt{\psi_a-\psi)(\psi_b-\psi)(\psi_c-\psi)(\psi+\psi_d)}}$. Thus, we obtain the following exact compacton solution family of system (1.7):

$$\phi(\xi) = \left(\psi_b - \frac{\psi_b - \psi_c}{1 - \hat{\alpha}_5^2 \text{sn}^2(\Omega_5\xi, k}\right)^{\frac{1}{2}}, \quad \xi \in (-\xi_0, \xi_0), \tag{2.15}$$

where $\hat{\alpha}_5^2 = \frac{\psi_c+\psi_d}{\psi_b+\psi_d}, \Omega_5 = \frac{1}{2}\omega_0\sqrt{(\psi_a - \psi_c)(\psi_b + \psi_d)}$ $k^2 = \frac{\hat{\alpha}_5^2(\psi_a-\psi_b)}{\psi_a-\psi_c}$ and $\xi_0 = \frac{1}{\Omega_4}\sqrt{\frac{\psi_c}{\hat{\alpha}_4^2\psi_b}}$.

Corresponding to the right homoclinic orbit to the equilibrium point $E_1(\phi_1, 0)$ defined by $H_1(\phi, y) = h_1$, in Fig.1 (g), now (2.5) can be written as

$$\omega_0 \xi = \int_{\psi_M}^{\psi} \frac{d\psi}{(\psi - \psi_1)\sqrt{(\psi_M - \psi)(\psi + \psi_d)}}.$$

Hence, it gives rise to the solitary wave solution as follows:

$$\phi(\xi) = \left(\psi_1 + \frac{2(\psi_M - \psi_1)(\psi_1 + \psi_d)}{(\psi_M + \psi_d)\cosh\left(\omega_0 \sqrt{(\psi_M - \psi_1)(\psi_1 + \psi_d)}\xi\right) - (\psi_M - \psi_d - 2\psi_1)} \right)^{\frac{1}{2}}. \tag{2.16}$$

3. Case II: $a > 0, \gamma^2 - \alpha^2 + 4a\omega > 0, 2ab_2 + \alpha\beta + \beta\gamma > 0, b_3 < 0$

In this section, we assume that $a > 0, \gamma^2 - \alpha^2 + 4a\omega > 0, 2ab_2 + \alpha\beta + \beta\gamma > 0, b_3 < 0$, which is equivalent to $a > 0, \lambda > 0, \sigma > 0, b_3 < 0$.

3.1. Phase portraits of system (1.7) for Case II

For a fixed parameter group $a > 0, \lambda > 0, \sigma > 0, b_3 < 0$, similar to the discussion in section 2, by varying the parameter b_1, the function $F(\phi)$ may have two or three positive zeros ϕ_j. Using the information in section 2 to do qualitative analysis, we have the following bifurcations of the phase portraits of system (1.7) shown in Fig.4. It should be noted that we take fixed parameter group: $(a, \lambda, \sigma, b_3) = (1, 7.8, 3.9, -0.45)$ in Fig.4. In this case, $F_4^M = 7.27571243, F_4^m = -13.0850874, \hat{b}_1 = 3.5645$.

3.2. Exact parametric representations of the orbits given by Fig.4

We see from (1.8) that

$$\begin{aligned} y^2 &= \frac{1}{\phi^2}\left(h\phi^2 - \frac{1}{a}\left(\frac{1}{3}b_3\phi^8 + \frac{1}{2}\hat{b_2}\phi^6 - \lambda\phi^4 + b_1\right)\right) \\ &= \frac{|b_3|}{3a\phi^2}\left(-\frac{3b_1}{|b_3|} + \frac{3ah}{|b_3|}\phi^2 + \frac{3\lambda}{|b_3|}\phi^4 - \frac{3\sigma}{2|b_3|}\phi^6 + \phi^8\right). \end{aligned}$$

Thus, by using the first equation of system (1.7), we have

$$\omega_1 \xi \equiv \sqrt{\frac{4|b_3|}{3a}}\xi = \int_{\psi_0}^{\psi} \frac{d\psi}{\sqrt{-\frac{3b_1}{|b_3|} + \frac{3ah}{|b_3|}\psi + \frac{3\lambda}{|b_3|}\psi^2 - \frac{3\sigma}{2|b_3|}\psi^3 + \psi^4}}, \tag{3.1}$$

where $\psi = \phi^2$. Applying (3.1), we can calculate the exact parametric representations of the orbits given by Fig.4.

(i) Fig.4 (b). In this case, we have $\phi_1 = \phi_2, h_1 = h_2$.

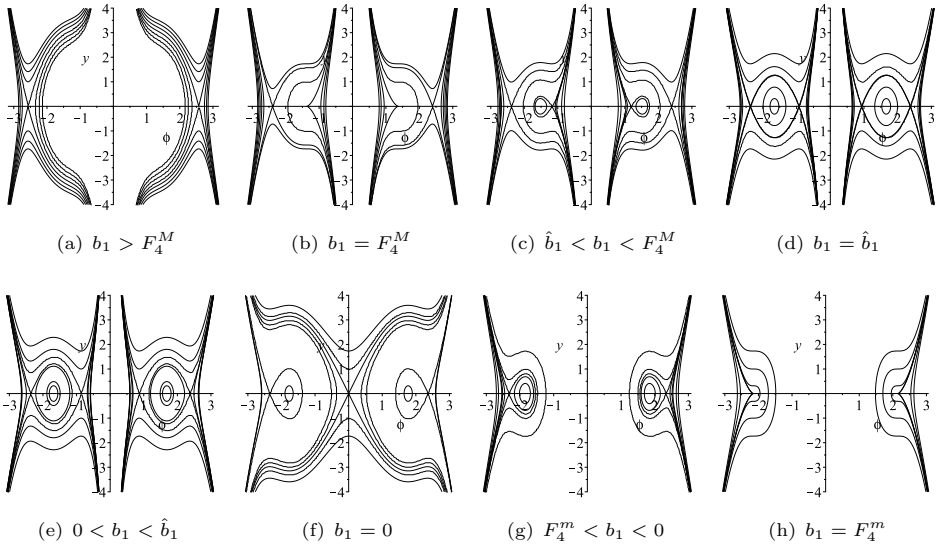

(a) $b_1 > F_4^M$ (b) $b_1 = F_4^M$ (c) $\hat{b}_1 < b_1 < F_4^M$ (d) $b_1 = \hat{b}_1$

(e) $0 < b_1 < \hat{b}_1$ (f) $b_1 = 0$ (g) $F_4^m < b_1 < 0$ (h) $b_1 = F_4^m$

Figure 4. The bifurcations of phase portraits of system (1.7) as b_1 is varied.

Corresponding to the right stable manifold of the cusp equilibrium point $E(\phi_1, 0)$ defined by $H_1(\phi, y) = h_1$, (3.1) reduce to $\omega_1\xi = \int_0^\psi \frac{d\psi}{(\psi_1-\psi)\sqrt{(\psi_a-\psi)(\psi_1-\psi)}}$. Hence, we have the following parametric representation:

$$\phi(\xi) = \left(\psi_1 - \frac{4(\psi_a-\psi_1)}{4+(\psi_a-\psi_1)^2\omega_1^2(\xi+\xi_{02})^2}\right)^{\frac{1}{2}}, \quad \xi \in (0,\infty), \tag{3.2}$$

where $\xi_{02} = \frac{2\sqrt{\psi_a\psi_1}}{\omega_1(\psi_a-\psi_1)\psi_1}$.

Corresponding to the right two open orbit families which tend to the singular straight line $\phi = 0$ when $|y| \to |\infty|$, defined by $H_1(\phi, y) = h, h \in (h_1, h_3)$ in Fig.4 (b), now (3.1) can be written as $\omega_1\xi = \int_\psi^{\psi_b} \frac{d\psi}{\sqrt{(\psi_a-\psi)(\psi_b-\psi)[(\psi-\tilde{b}_1)^2+\tilde{a}_1^2]}}$. It gives rise to the following compacton solution family of system (1.7):

$$\phi(\xi) = \left(\breve{\alpha}_1 + \frac{\breve{\beta}_1}{1+\hat{\alpha}_6\mathrm{cn}(\Omega_6\xi, k)}\right)^{\frac{1}{2}}, \quad \xi \in (-\xi_{03}, \xi_{03}), \tag{3.3}$$

where

$$\breve{\alpha}_1 = \frac{\psi_a B_1 - \psi_b A_1}{B_1 - A_1}, \quad \breve{\beta}_1 = \frac{2A_1B_1(1-\psi_b)}{A_1^2 - B_1^2}, \quad \hat{\alpha}_2 = \frac{A_1 - B_1}{A_1 + B_1},$$
$$k^2 = \frac{(\psi_a-\psi_b)^2 - (A_1-B_1)^2}{4A_1B_1}, \quad \Omega_6 = \omega_1\sqrt{A_1B_1}, \quad A_1^2 = (\psi_a - \tilde{b}_1)^2 + \tilde{b}_1^2,$$
$$B_1^2 = (\psi_b - \tilde{b}_1)^2 + \tilde{a}_1^2, \quad \xi_{03} = \frac{1}{\Omega_6}\mathrm{cn}^{-1}\left(\frac{1}{\hat{\alpha}_2}\left(1 + \frac{\breve{\beta}_1}{\breve{\alpha}_1}\right)\right).$$

(ii) Fig.4 (c). In this case, with h is varied, the changes of level curves defined by $H_1(\phi, y) = h$ are shown in Fig.5 (a)-(e).

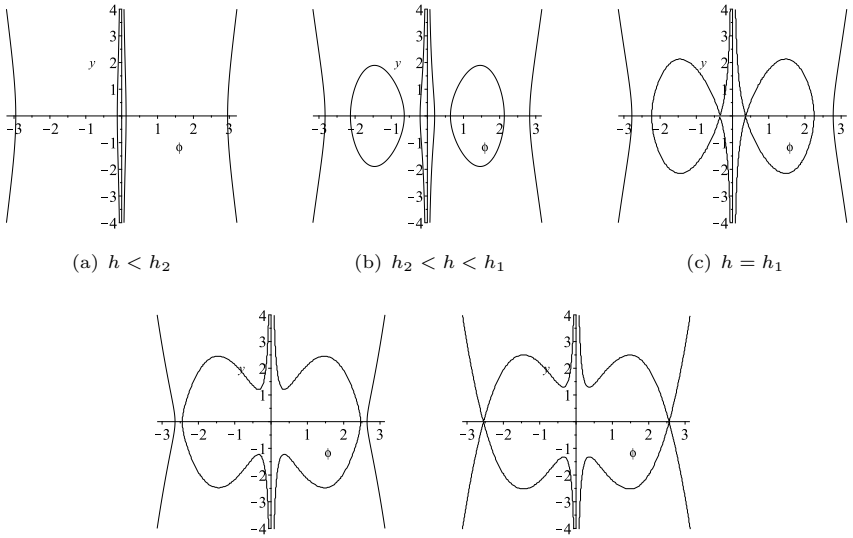

(a) $h < h_2$ (b) $h_2 < h < h_1$ (c) $h = h_1$

(d) $h_1 < h < h_3$ (e) $h = h_3$

Figure 5. The level curves $H_1(\phi, y) = h$ of system (1.7) as h is varied for $h_2 < h_1 < h_3$

When $h < h_2$, corresponding to the right open curve family defined by $H_1(\phi, y) = h$ (see Fig.5 (a)) which tends to the singular straight line $\phi = 0$ when $|y| \to |\infty|$, (3.1) can be written as $\omega_1\xi = \int_{\psi}^{\psi_b} \frac{d\psi}{\sqrt{(\psi_a-\psi)(\psi_b-\psi)[(\psi-\tilde{b}_1)^2+\tilde{a}_1^2]}}$. It gives rise to the same compacton solution family of system (1.7) as (3.3).

When $h_2 < h < h_1$, corresponding to the right open curve family defined by $H_1(\phi, y) = h$ which tends to the singular straight line $\phi = 0$ when $|y| \to |\infty|$, (3.1) can be written as $\omega_1\xi = \int_{\psi}^{\psi_d} \frac{d\psi}{\sqrt{(\psi_a-\psi)(\psi_b-\psi)(\psi_c-\psi)(\psi_d-\psi)}}$ and corresponding to the right closed curve family defined by $H_1(\phi, y) = h$ enclosing the equilibrium point $E_2(\phi_2.0)$ (see Fig.5 (b)), (3.1) can be written as $\omega_1\xi = \int_{\psi_c}^{\psi} \frac{d\psi}{\sqrt{(\psi_a-\psi)(\psi_b-\psi)(\psi-\psi_c)(\psi-\psi_d)}}$. Thus, we obtain a compacton solution family and a periodic solution family of system (1.7), respectively, as follows:

$$\phi(\xi) = \left(\psi_c - \frac{\psi_c - \psi_d}{1 - \hat{\alpha}_7^2 \mathrm{sn}^2(\Omega_7\xi, k)}\right)^{\frac{1}{2}}, \quad \xi \in (-\xi_{04}, \xi_{04}), \tag{3.4}$$

where

$$\hat{\alpha}_7^2 = \frac{\psi_a - \psi_d}{\psi_a - \psi_c}, \quad \Omega_7 = \frac{1}{2}\omega_1\sqrt{(\psi_a - \psi_c)(\psi_b - \psi_d)},$$
$$k^2 = \frac{\hat{\alpha}_7^2(\psi_b - \psi_c)}{\psi_b - \psi_d}, \quad \xi_{04} = \frac{1}{\Omega_7}\mathrm{sn}^{-1}\sqrt{\frac{\psi_d}{\psi_c\hat{\alpha}_7^2}}.$$

And

$$\phi(\xi) = \left(\psi_d + \frac{\psi_c - \psi_d}{1 - \hat{\alpha}_7^2 \mathrm{sn}^2(\Omega_7\xi, k)}\right)^{\frac{1}{2}}, \tag{3.5}$$

where $\hat{\alpha}_7^2=\frac{\psi_a-\psi_c}{\psi_b-\psi_d}, \Omega_7=\frac{1}{2}\omega_1\sqrt{(\psi_a-\psi_c)(\psi_b-\psi_d)}, k^2=\frac{\hat{\alpha}_7^2(\psi_a-\psi_d)}{\psi_a-\psi_c}$.

When $h=h_1$, corresponding to the right homoclinic orbit to the saddle point $E_1(\phi_1,0)$ defined by $H_1(\phi,y)=h_1$ (see Fig.5 (c)), (3.1) can be written as $\omega_1\xi=\int_{\psi}^{\psi_M}\frac{d\psi}{(\psi-\psi_1)\sqrt{\psi_a-\psi)(\psi_M-\psi)}}$. It gives rise to the following solitary wave solution of system (1.7):

$$\phi(\xi)=\left(\psi_1+\frac{2(\psi_a-\psi_1)(\psi_M-\psi_1)}{(\psi_a-\psi_M)\cosh\left(\omega_1\sqrt{(\psi_a-\psi_1)(\psi_M-\psi_1)}\xi\right)+(\psi_a+\psi_M-2\psi_1)}\right)^{\frac{1}{2}}. \tag{3.6}$$

When $h_1<h<h_3$, corresponding to the right open curve family defined by $H_1(\phi,y)=h$ which tends to the singular straight line $\phi=0$ when $|y|\to|\infty|$ (see Fig.5 (d)), it gives rise two a compacton solution family with the same parametric representation as (3.3).

When $h=h_3$, corresponding to the stable manifold of the saddle point $E_3(\phi_3,0)$, (3.1) can be written as $\omega_1\xi=\int_0^{\psi}\frac{d\psi}{(\psi_3-\psi)\sqrt{(\psi-b_2)^2+a_2^2}}$. Thus, we have the following parametric representation:

$$\phi(\xi)=\left(\psi_3-\frac{2A_2}{P_2\cosh_q\left(\omega_1\sqrt{A_2}\xi\right)+B_2}\right)^{\frac{1}{2}}, \tag{3.7}$$

where

$$A_2=a_2^2+b_2^2+\psi_3^2+2b_2\psi_3,\quad B_2=2(b_2+\psi_3),$$
$$P_2=\frac{2\sqrt{A_2(a_2^2+b_2^2)}-B_2\psi_3+2A_2}{\psi_3},\quad q=\frac{-4a_2^2}{P_2^2}.$$

(iii) Fig.4 (d). In this case, we have $h_1=h_3$.

When $h<h_2$ and $h_2<h<h_1=h_3$, we have the same exact solutions as (3.3), (3.4) and (3.5).

When $h=h_1=h_3$, corresponding to the right heteroclinic loop connecting the equilibrium point $E_1(\phi_1,0)$ and $E_3(\phi_3,0)$ defined by $H_1(\phi,y)=h_1$ (see Fig.5 (e)), now (3.1) becomes $\omega_1\xi=\int_{\psi_2}^{\psi}\frac{d\psi}{(\psi_3-\psi)(\psi-\psi_1)}$. Hence, we have the following kink and anti-kink wave solutions of system (1.7):

$$\phi(\xi)=\left(\frac{\psi_1+\psi_3e^{\omega_3(\xi+\hat{\xi}_0)}}{1+e^{\omega_3(\xi+\hat{\xi}_0)}}\right)^{\frac{1}{2}}, \tag{3.8}$$

where $\omega_3=(\psi_3-\psi_1)\omega_1, \hat{\xi}_0=\frac{1}{\omega_1}\ln\left(\frac{\psi_2-\psi_1}{\psi_3-\psi_2}\right)$.

(iv) Fig.5 (e). In this case, with h is varied, the changes of level curves defined by $H_1(\phi,y)=h$ are shown in Fig.6 (a)-(e).

When $h<h_2$ and $h_2<h<h_3$, we have the same exact solutions as (3.3), (3.4) and (3.5).

When $h=h_3$, corresponding to the right homoclinic orbit to the saddle point $E_3(\phi_1,0)$ defined by $H_1(\phi,y)=h_3$ (see Fig.6 (c)), (3.1) can be written as $\omega_1\xi=$

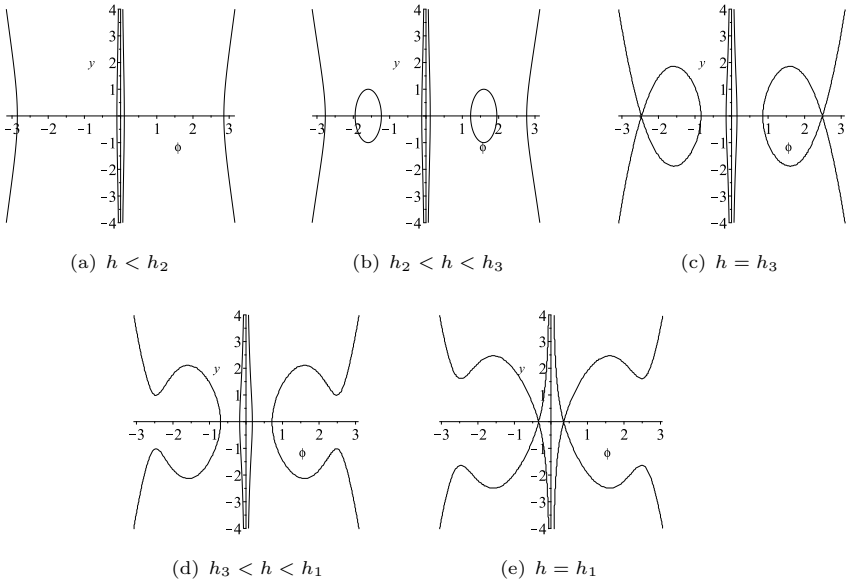

(a) $h < h_2$ (b) $h_2 < h < h_3$ (c) $h = h_3$

(d) $h_3 < h < h_1$ (e) $h = h_1$

Figure 6. The level curves defined by $H_1(\phi, y) = h$ of system (1.7) as h is varied for $h_2 < h_3 < h_1$

$\int_{\psi_M}^{\psi} \frac{d\psi}{(\psi_3-\psi)\sqrt{\psi-\psi_M)(\psi-\psi_d)}}$. It gives rise to the following solitary wave solution of system (1.7):

$$\phi(\xi)=\left(\psi_3-\frac{2(\psi_3-\psi_d)(\psi_3-\psi_M)}{(\psi_M-\psi_d)\cosh\left(\omega_1\sqrt{(\psi_3-\psi_d)(\psi_3-\psi_M)}\xi\right)-(\psi_M+\psi_d-2\psi_3)}\right)^{\frac{1}{2}}. \tag{3.9}$$

When $h_3 < h < h_1$, corresponding to the right open curve family defined by $H_1(\phi, y) = h$ which tends to the singular straight line $\phi = 0$ when $|y| \to |\infty|$ (see Fig.6 (d)), it gives rise two a compacton solution family with the same parametric representation as (3.3).

When $h = h_1$, corresponding to the stable manifold of the saddle point $E_1(\phi_1, 0)$ (see Fig.6 (e)), (3.1) can be written as $\omega_1\xi = \int_0^{\psi} \frac{d\psi}{(\psi_1-\psi)\sqrt{(\psi-b_3)^2+a_3^2}}$. Thus, we have the following parametric representation:

$$\phi(\xi) = \left(\psi_1 - \frac{2A_3}{P_3\cosh_q\left(\omega_1\sqrt{A_3}\xi\right)+B_3}\right)^{\frac{1}{2}}, \tag{3.10}$$

where

$$A_3=a_3^2+b_3^2+\psi_1^2+2b_3\psi_1, \quad B_3=2(b_3+\psi_1),$$
$$P_3=\frac{2\sqrt{A_3(a_3^2+b_3^2)}-B_3\psi_1+2A_3}{\psi_1}, \quad q=\frac{-4a_3^2}{P_3^2}.$$

References

[1] S. S. Afzal, M. Younis and S. T. R. Rizvi, *Optical dark and dark-singular solitons with anti-cubic nonlinearity*, Optik, 2017, 147, 27–31.

[2] K. S. Al-Ghafri1 and E. V. Krishnan, *Optical solitons in metamaterials dominated by anti-cubic nonlinearity and Hamiltonian perturbations*, Int. J. Appl. Comput. Math., 2020, 6(5), 144.

[3] A. H. Arnous, M. Ekici, S. P. Moshokoa et al, *Solitons in nonlinear directional couplers with optical metamaterials by trial function scheme*, Acta Phys. Polonica A., 2017, 132(4), 1399–1410.

[4] A. Biswas, R. Kaisar, K. R. Khan et al, *Bright and dark solitons in optical metamaterials*, Optik, 125(13), 3299–3302.

[5] A. Biswas, A. Mirzazadeh, M. Savescu et al, *Singular solitons in optical metamaterials by ansatz method and simplest equation approach*, J. of Modern Optics, 2014, 61(19), 1550–1555.

[6] P. F. Byrd and M. D. Fridman, *Handbook of Elliptic Integrals for Engineers and Sciensists*, Springer, Berlin, 1971.

[7] M. Ekici, A. Sonmezoglu, Q. Zhou et al, *Analysis of optical solitons in nonlinear negative-indexed materials with anti-cubic nonlinearity*, Opt. Quantum Electron., 2018, 50(2), 75.

[8] M. Foroutan, J. Manafian and A. Ranjbaran, *Solitons in optical metamaterials with anti-cubic law of nonlinearity by generalized $\frac{G'}{G}$-expansion method*, Optik, 2018, 162, 86–94.

[9] M. Foroutan, J. Manafian and I. Zamanpour, *Solitonwave solutions in optical metamaterials with anti-cubic law of nonlinearity by ITEM*, Optik, 2018, 164, 371–379.

[10] Y. Fu and J. Li, *Exact stationary-wave solutions in the standard model of the Kerr-nonlinear optical fiber with the bragg grating*, J. Appl. Anal, Comput., 2017, 7(3), 1177–1184.

[11] A. A. Kader, M. A. Latif and Q. Zhou, *Exact optical solitons in metamaterials with anti-cubic law of nonlinearity by Lie group method*, Opt. Quantum Electron, 2019, 51(1), 30.

[12] J. Li, *Geometric properties and exact travelling wave solutions for the generalized Burger-Fisher equation and the Sharma-Tasso-Olver equation*, J. Nonl. Mod. Anal., 2019, 1(1), 1–10.

[13] J. Li, *Singular Nonlinear Traveling Wave Equations: Bifurcations and Exact Solutions*, Science Press, Beijing, 2013.

[14] J. Li and G. Chen, *Bifurcations of travelling wave solutions for four classes of nonlinear wave equations*, Int. J. Bifurcat. Chaos, 2005, 15(12), 3973–3998.

[15] J. Li and G. Chen, *On a class of singular nonlinear traveling wave equations*, Int. J. Bifurcat. Chaos, 2007, 17(11), 4049–4065.

[16] J. Li and M. Han, *Exact peakon solutions given by the generalized hyperbolic functions for some nonlinear wave equations*, J. Appl. Anal, Comput., 2020, 10(4), 1708–1719.

[17] J. Li, Y. Zhang and X. Zhao, *On a class of singular nonlinear traveling wave equations (II): an example of GCKdV equations*, Int. J. Bifurcat. Chaos, 2009, 19(6), 1955–2007.

[18] J. Li, W. Zhou, and G. Chen, *Understanding peakons, periodic peakons and compactons via a shallow water wave equation*, Int. J. Bifurcat. Chaos, 2016, 26(12), 1650207.

[19] A. Sonmezoglu, M. Yao, M. Ekici et al, *Explicit solitons in the parabolic law nonlinear negative-index materials*, Nonlinear Dynam., 2016, 88(1), 1–13.

[20] Y. Xiang, X. Dai, S. Wen et al, *Controllable Raman soliton self-frequency shift in nonlinear metamaterials*, Phys. Rev. A, 2011, 84(3), 2484–2494.

[21] Y. Xu, P. Pablo Suarez, D. Milovic et al, *Raman solitons in nanoscale optical waveguides, with metamaterials, having polynomial law non-linearity*, J. Mod. Optic., 2016, 63(S3), S32–S37.

[22] Y. Zhou and J. Li, *Exact solutions and dynamics of the Raman soliton model in nanoscale optical waveguides, with metamaterials, having polynomial law nonlinearity*, Int. J. Bifurcat. Chaos, 2017, 27(12), 1750188.

[23] Q. Zhou, L. Liu, Y. Liu et al, *Exact optical solitons in metamaterials with cubicšCquintic nonlinearity and third-order dispersion*, Nonlinear Dynam., 2015, 80(3), 1365–1371.

[24] Q. Zhou, M. Mirzazadeh, M. Ekici et al, *Analytical study of solitons in non-Kerr nonlinear negative index materials*, Nonlinear Dynam., 2015, 86(1), 623–638.

[25] Y. Zhou and J. Zhuang, *Bifurcations and exact eolutions of the Raman soliton model in nanoscale optical waveguides with metamaterials*, J. Nonl. Mod. Anal., 2021, 3(1), 145–165.